Published in final edited form as:
J Cell Biochem. 2012 June ; 113(6): 1998–2008. doi:10.1002/jcb.24069.

Arachidonate 5 Lipoxygenase Expression in Papillary Thyroid Carcinoma Promotes Invasion via MMP-9 Induction

Nicolas T. Kummer[1], **Theodore S Nowicki**[1], **Jean Paul Azzi**[2], **Ismael Reyes**[1], **Codrin Iacob**[2], **Suqing Xie**[3], **Ismatun Swati**[3], **Nina Suslina**[4], **Stimson Schantz**[4], **Raj K. Tiwari**[1,4], and **Jan Geliebter**[*,1,4]

[1]Department of Microbiology & Immunology, New York Medical College, Valhalla, NY, USA

[2]Department of Pathology, The New York Eye & Ear Infirmary, New York, NY, USA

[3]Department of Pathology, New York Medical College, Valhalla, NY, USA

[4]Department of Otolaryngology, New York Medical College, Valhalla, NY, USA

Abstract

Arachidonate 5-lipoxygenase (ALOX5) expression and activity has been implicated in tumor pathogenesis, yet its role in papillary thyroid carcinoma (PTC) has not been characterized. ALOX5 protein and mRNA were upregulated in PTC compared to matched, normal thyroid tissue, and ALOX5 expression correlated with invasive tumor histopathology. Evidence suggests that PTC invasion is mediated through the induction of matrix metalloproteinases (MMPs) that can degrade and remodel the extracellular matrix (ECM). A correlation between MMP-9 and ALOX5 protein expression was established by immunohistochemical analysis of PTC and normal thyroid tissues using a tissue array. Transfection of ALOX5 into a PTC cell line (BCPAP) increased MMP-9 secretion and cell invasion across an ECM barrier. The ALOX5 product, 5(S)-hydroxyeicosatetraenoic acid also increased MMP-9 protein expression by BCPAP in a dose-dependent manner. Inhibitors of MMP-9 and ALOX5 reversed ALOX5-enhanced invasion. Here we describe a new role for ALOX5 as a mediator of invasion via MMP-9 induction; this ALOX5/MMP9 pathway represents a new avenue in the search for functional biomarkers and/or potential therapeutic targets for aggressive PTC.

Keywords

Arachidonate 5-Lipoxygenase; Matrix Metalloproteinase-9; Tumor Invasion; 5-HETE; Extracellular Matrix; Papillary Thyroid Carcinoma

Introduction

Papillary thyroid carcinoma (PTC) constitutes ~80% of all thyroid cancers(Ries LAG, 2008) and typically arises from a gain-of-function mutation in the RET, RAS or BRAF genes which comprise a linear signaling cascade resulting in activation of the mitogen-activated protein kinase/extracellular signal-regulated kinase (MAPK/ERK) system.(Melillo et al., 2005) Currently, thyroidectomy remains the main treatment option for PTC and post-surgical management is associated with significant morbidity, exposing patients to surgical risk and requiring lifelong hormone replacement therapy. Recurrent or persistent disease

[*]Correspondence to: Jan Geliebter Ph.D. Department of Microbiology and Immunology, New York Medical College, BSB-311, 95 Grasslands Road, Valhalla NY 10595; jan_geliebter@nymc.edu; phone: (914) 594-4873; fax (914) 594-4405.

occurs in up to 40% of thyroidectomy cases, with a poor prognosis when aggressive cancer is evident.(Vasko and Saji, 2007) Biomarkers for the early identification of aggressive PTC and identification of new therapeutic targets could lead to better disease management and decreased morbidity.

ALOX5 is a central regulator of acute inflammation and has been implicated in cancer pathogenesis.(Hanaka et al., 2002; Luo et al., 2003; Luo et al., 2004) The most characterized function of ALOX5 in leukocytes is the conversion of arachidonic acid (AA) and other fatty acids to bioactive compounds such as 5(S)-hydroxyeicosatetraenoic acid (5-HETE), leukotriene B4 (LTB4), and other leukotrienes.(Bednar et al., 1987; Bokoch and Reed, 1981; Goldyne et al., 1984; Randall et al., 1980) There is a growing body of evidence suggesting that ALOX5 has a role in tumorigenesis, and may be a potential therapeutic target and biomarker. ALOX5 expression by cancer and stromal cells has been demonstrated in a variety of tumors in studies based on clinical samples, and validated in experimental models. (Ding et al., 2003; Ghosh and Myers, 1997; Marks et al., 2000; Pires de Miranda et al., 2003) Tissue culture models of prostate and breast cancer demonstrate that *in vitro* inhibition of ALOX5 and/or ALOX5 activating protein (FLAP) can induce apoptosis in cancer cells.(Avis et al., 2001; Ding et al., 2003; Ghosh, 2003; Tong et al., 2002) Similar studies show that the addition of 5-HETE, or AA to cancer cell lines can increase cell viability and growth *in vitro*.(Ghosh and Myers, 1997; Zeng et al., 2002) To date, there have been no significant studies investigating a mechanistic role between ALOX5 function and tumor invasion.

Invasion in cancer is mediated through a complex network of extracellular proteases which can degrade the extracellular matrix (ECM) and modify the tumor microenvironment. Matrix metalloproteinases (MMPs) and their inhibitors, tissue inhibitors of matrix metalloproteinase (TIMPs), have been shown to play central roles in tumor invasion by degrading ECM, regulating other proteases, and producing signaling molecules in the extracellular environment.(Chambers and Matrisian, 1997; Egeblad and Werb, 2002; Pires de Miranda et al., 2003; Sato et al., 1994; Westermarck and Kahari, 1999) MMP-9 (gelatinase B) is a secreted 92-kDa type IV collagenase which is expressed and secreted by invasive tumors, and has been implicated in PTC pathogenesis.(Egeblad and Werb, 2002; Opdenakker et al., 2001; Stuve et al., 1996)

While previous studies support a role of ALOX5 in tumor growth, there are no mechanistic studies demonstrating how ALOX5 or 5-HETE mediate tumor invasion, and there is only limited evidence correlating ALOX5 expression and activity with invasiveness in clinical samples.(Soumaoro et al., 2006) Additionally, inflammatory cytokines have been shown to regulate the expression of MMP-9; however, there is no evidence linking ALOX5 activity with MMP-9 regulation. Here, we explore the functional role of ALOX5 expression in PTC, and demonstrate that ALOX5 expression levels positively correlate with aggressive tumor histopathology. Furthermore, we demonstrate a new functional role for ALOX5 in MMP-9 regulation and tumor invasion in an experimental model of human PTC.

Materials and Methods

Patient Tissue Samples

PTC and matched, normal thyroid tissues were obtained from patients at New York Eye and Ear Infirmary and Westchester Medical Center in accordance with institutional IRB-approved clinical protocols. Samples contained > 90% PTC or >90% normal appearing tissue, as confirmed by histology. In addition, clinical pathology reports were collected for gathering data on TNM stage, tumor grade, age, sex, tumor size and location of disease. Tumors were also graded for invasive histopathology on a scale of 1 to 3 using our Tumor

Invasive Score (TIS): TIS-1 = no evidence of invasive disease, TIS-2 = lymphatic spread and/or involvement of the capsule without extra-thyroidal extension, TIS-3 = extra-glandular extension and/or spread to local tissue.

Cell Lines and Culture Conditions

The human PTC cell line BCPAP was purchased from DSMZ (Braunschweig, Germany). BCPAP are BRAFV600E positive PTC cells derived from the tumor of a 76-year-old patient with nodal metastasis.(Fabien et al., 1994) The cell line was validated by sequence analysis for the BRAFV600E mutation (data not shown). Cell lines were maintained in a humidified incubator at 37°C and 5% CO_2 in RPMI 1640 (Mediatech Inc, Manassas, VA) supplemented with 10 mg/mL L-glutamine (Mediatech Inc.), 100 IU penicillin, 100 mg/mL streptomycin (Mediatech Inc), and 10% fetal bovine serum (Sigma, St. Louis, MI) unless specified otherwise. Inhibition of ALOX5, MMP-9 and MMPs were achieved with the addition of Zileuton (Cayman Chemicals, Ann Arbor MI), anti-MMP-9 antibody (Calbiochem CAT# 444236, San Diego, CA), and 1,10 Phenanthroline (1,10 PE, Invitrogen, Carlsbad, CA), respectively.

Transfection of ALOX5-pcDNA3.1(−) in BCPAP

The neomycin resistant pcDNA3.1(−) plasmid containing the ALOX5 coding region was kindly provided by Dr. Thomas Brock (University of Michigan Medical School). pcDNA3.1(−) plasmids containing the ALOX5 gene, or the empty vector control, were transfected into BCPAP cells (referred to as ALOX5-BCPAP and pcDNA-BCPAP, respectively) in 6 well plates using FuGENE^{tm} 6 Transfection Reagent (Roche Molecular Biochemicals, Indianapolis, IN) according to manufacturer's protocol. Cells were grown under standard culture conditions with the addition of 1 mg/mL G418 (Promega, Madison, WI). ALOX5 mRNA transcription was quantified by real-time RT-PCR (Figure 3A) and ALOX5 protein was determined by western blot analysis (Figure 3B).

RNA Extraction and Quantitative Real-Time RT-PCR

RNA was isolated using TRizol® (Invitrogen) according to manufacturer's protocol. Quantitative real-time RT-PCR was performed using an ABI 7900HT System (ABI, Foster City, CA.). Target transcripts were quantified using SYBR®Green One-Step qRT-PCR (Invitrogen) for ALOX5 (forward: 5'-TGGAATGACTTCGCCGACTTTGAG-3', reverse: 5'-TAGCCAAACATCAGGTCTTCCTGC-3') and glyceraldehyde-3-phosphate dehydrogenase (GAPDH) mRNA (forward: 5'-ACCACAGTCCATGCCATCAC-3', reverse: 5'-TCCACCACCCTGTTGCTGTA-3') with quantitative standards.

ALOX5 and MMP-9 Immunohistochemistry

All IHC was performed on serial sections of a human thyroid cancer tissue array (Cybrdi, Rockville, MD). ALOX5 IHC was performed by Charles Rivers Laboratories, Pathology Services (Wilminton, MA). Sections were processed under pressure in Declere solution (Sigma), followed by H_2O_2 and microwave antigen retrieval. Sections were blocked with 1.5% goat serum, 5% milk and 1% BSA, followed by 1:50 dilution of ALOX5 primary antibody (BD Transduction Laboratories) and 1:1000 dilution of goat anti-mouse secondary antibody (Jackson ImmunoResearch Laboratories, West Grove, PA) and processed with Vectastain ABC reagents, (Vector Lab, Burlingame CA). MMP-9 IHC was carried out in-house; after xylene deparaffinization and antigen retrieval (10mM Sodium Citrate, 0.05% Tween 20, pH 6.0) at 100°C for 20 minutes, sections were blocked in Blocking Solution (Vectistain ABC KIT). A 1:200 dilution of anti-MMP-9 antibody (Cell Signaling, Cat# 3852, rabbit polyclonal Ab) in blocking solution was used for primary antibody binding, and resolved with Vectastain ABC reagents. Sections were graded 0–4 for ALOX5and MMP-9

staining as follows: 1= weak staining of less than 50% of cells (referring to the total number of tumor or follicle cells), 2= weak staining of greater than 50% cells, 3=strong staining of greater than 50%, and 4 = the strongest staining of greater than 50% of cells. The sample and IHC stain identities were blinded to two independent pathologists who scored the section.

Cell Growth and Viability

Growth curves were determined using standard trypan-blue exclusion method for 5 time points collected over a period of 120 hours for ALOX5-BCPAP, and pcDNA BCPAP, in triplicate under standard conditions. Dose responses to AA and Zileuton were determined by the metabolism of the tetrazolium salt, 3'-[1-[(phenylamino)-carbonyl]-3,4-tetrazolium]-bis(4-methoxy-6-nitro)benzene-sulfonic acid hydrate (XTT) as described by *Roehm et al.* (Roehm et al., 1991) In brief, 2,500 cells were plated (in replicates of 6) in 96 well plates in complete media for 24 hours, followed by media replacement with the experimental conditions (no treatment, 0.01, 0.10, 1.00, 2.50, and 5.00 μM AA in serum reduced media-1% FBS supplemented RPMI; or, 7.5, 10, 25, 50, and 100 μM Zileuton in complete RPMI). XTT metabolism was assessed after 72 hours of incubation under standard conditions. Results were reported as a percentage of the no treatment control.

Laser Scanning Cytometry for Cell Cycle Determination

Ten thousand pcDNA-BCPAP or ALOX5-BCPAP cells were seeded onto chambered slides under standard conditions. Cells were fixed at 50% growth confluence and stored in methanol at 4°C until processing. Slides were washed twice in PBS for 5 minutes, stained with DAPI (Sigma) at a concentration of 2.8 μg/mL for 15 minutes and rinsed in PBS. Cover slips were mounted with antifade and analyzed for cell cycle distribution on an iCys system (Compucyte, Cambridge, MA).

Invasion and Migration Assay

Cellular invasion and migration were assessed in quadruplicate using the BD BioCoat^{tm} Tumor Invasion System (BD Bioscience, San Jose, CA). Cells were harvested at approximately 50% confluence, and 15,000 or 25,000 cells were plated per upper chamber in serum free RPMI, with 10% or 5% FBS supplemented RPMI in the lower chamber as chemoattractant. Fifty μM Zileuton, inhibitory anti-MMP9 antibody, or 200 μM 1,10 PE were added to the chambers, and incubated under standard tissue culture conditions for 22 hours. Invading and migrating cells were stained with 1% Toludine Blue. Images were acquired at 50X or 100X magnification by light microscopy, converted to 8-bit grey scale, optimized for contrast and threshold, and cells automatically counted using the ImageJ software.(Rasband) Percent invasion/migration for each replicate was calculated [(invading cells/migrating cells)*100]; P values were determined by Student t-test.

MMP Protein Array

Conditioned medium was prepared from pcDNA-BCPAP and ALOX5-BCPAP cells. Conditioned media were collected, and clarified by centrifugation at 1,000 g for 5 minutes. Secreted MMPs and TIMPs were assessed using a RayBio Human Matrix Metalloproteinase Antibody Array I (RayBio, Norcross, GA) according to manufacturer's protocol. The resulting autoradiographs were quantified by spot densitometry using the ImageJ software. (Rasband)

Western Blot Analysis

Western blot analysis was performed on serum-free conditioned media (SFCM) for MMP-9, and cell lysates for ALOX5 and beta-actin. SFCM was prepared from 700,000 cells seeded

in T-25 flasks, supplemented with 10 μM arachidonic acid (Cayman Chemicals), 0.1 μM 5-HETE, 1.0 μM 5-HETE, or ethanol (vehicle control). SFCM and cells were collected at 32 hours. For Western blot analysis of MMP-9, SFCM was concentrated by trichloroacetic acid (TCA) precipitation. Proteins were separated by 8% sodium dodecyl sulfate polyacrylamide gel electrophoresis (SDS-PAGE) following standard Laemmli conditions.(Laemmli, 1970) Membranes were blocked in 6% milk in Tris-buffered saline plus Tween-20 (TBST-20 mM Tris, 500 mM NaCl pH 7.5, 0.05% Tween-20) for 1 hour at room temperature, incubated with a 1:1000 dilution of anti-MMP9 antibody in 6% milk-TBST overnight, washed 3 times for 5 minutes each in TBST, and incubated with secondary antibody at a 1:15,000 dilution (Peirce, Rockford, IL) in 1% milk TBST for 2 hours at room temperature. Membranes were washed three times for 5 minutes in TBST, and visualized by Pierce ECL Western Blotting Substrate. ALOX5, and beta-actin Western blot analysis were performed on cell lysates. Twenty μg of protein were fractionated by 10% SDS-PAGE and processed as described above with the following modifications. A 1:200 dilution of anti-ALOX5 mouse monoclonal antibody (BD Transduction Laboratories CAT# F58420-150, San Jose CA), or a 1:1,000 dilution of anti-beta-actin rabbit monoclonal antibody (Cell Signaling CAT# 13E5, Danvers, MA), in 3% milk TBST were used. The optical density of the autoradiographic images were calculated with ImageJ (Rasband) using the following formula: OD = band area * LOG [(average background pixel intensity-average black control pixel intensity)/average band pixel intensity – average black control pixel intensity)]

Statistical Analysis

Data was analyzed as described using Microsoft Excel (Redmond, WA), GraphPad Prism 5 (La Jolla, CA) or NCSS (Kaysville, UT). All bar graphs represent mean values ±standard error of the mean (SEM), unless otherwise specified.

Results

ALOX5 Expression in PTC and Correlation with Invasive Histopathology

To investigate ALOX5 expression in invasive PTC, ALOX5 mRNA was quantified by real-time RT-PC in 17 pairs of PTC and matched, normal thyroid tissue. ALOX5 expression in PTC was significantly increased by 12.6 fold, compared to the matched normal thyroid tissue (Figure 1A). Additionally, the fold change in ALOX5 mRNA for each matched pair were calculated and correlated positively with TIS (Figure 1B), suggesting aggressive PTC is associated with increased ALOX5 expression (Spearman correlation r_S=0.74 p=0.0007). The BRAFV600E mutation is known to be associated with aggressive disease and ALOX5 expression trended upwards in BRAFV600E positive samples but did not reach statistical significance (BRAF wt 12.60 ± 4.78 fold change; BRAFV600E 32.56 ±12.11 fold change; p=0.05), further strengthening a role between ALOX5 and aggressive disease.

ALOX5 is a bioactive molecule involved in stimulating acute inflammation through the metabolism of AA to active compounds which are involved in cell signaling. (Jakobsson et al., 1992) Preliminary lipidomic studies by quantitative LC-MS/MS demonstrated the presence of the AA derived ALOX5 product, 5-HETE, at a biologically relevant concentration of 13.47 ± 4.26 pg/mg tissue (data not shown).(Yang et al., 2006)

ALOX5 Activity and Cell Dynamics in BCPAP

ALOX5, 5-HETE and AA can confer a growth advantage in tissue culture models of prostate and breast cancer. (Avis et al., 2001; Ghosh, 2003; Ghosh and Myers, 1997; Tong et al., 2002). To determine the effect of these molecules in our PTC model; cell growth, viability and cell cycle characteristics were evaluated in the BRAFV600E positive cell line, BCPAP, transfected with an ALOX5 expression vector (ALOX5-BCPAP), or an empty,

control vector (pcDNA-BCPAP). Transfectants were validated for vector insertion by real-time PCR(data not shown), ALOX5 mRNA expression by real-time RT-PCR, protein expression (Figure 2), and ALOX5 activity by LC-MS/MS(data not shown). ALOX5-BCPAP had 156-fold increase in ALOX5 mRNA expression compared to control (Figure A) and increased ALOX5 protein levels, determined by western blot analysis (Figure 2B).

The transfection of ALOX5/empty vector into BCPAP allows for phenotypic comparisons to a genetically identical control, and the direct characterization of ALOX5 upregulation in this PTC model. ALOX5 overexpression, and the addition of Zileuton, were found to have no effects on the cell cycle or growth dynamics, suggesting no significant role for ALOX5 activity in proliferation and survival. (Figure 3). The normal tissue concentration of AA in thyroid tissue is unknown; however, un-esterified AA is reported to have a physiologic range of the low μM in inflammatory tissues. Additionally, un-esterified-AA has been shown to be cytotoxic to some cell lines in the nM range. (Brash, 2001) Here, the addition of free AA showed no comparative effect on growth between cell lines, and was equally toxic at concentrations above 50 μM, consistent with the previous findings.

ALOX5 Mediated Invasion Across ECM

The invasive property of ALOX5-BCPAP and pcDNA-BCPAP (control) cells were determined using the BD BioCoat^{tm} Tumor Invasion System (BD Bioscience). This system utilizes Boyden chambers, containing a porous membrane (8 micron pores) which separates cells plated in the upper chamber from chemoatractant in the lower chamber. Cells have to migrate through the membrane pores to gain access to the chemoatractant. To investigate invasion, membranes are coated with a thin layer of Matrigel that acts as an ECM barrier to migration; cells have to actively degrade the Matrigel in order to migrate through the pores towards the chemoatractant. To control for any change in the rate of cell migration (independent of invasion), migration is also assessed in parallel in chambers without Matrigel. Invasion is reported as the percent of cells invading through the Matrigel divided by the number of cells migrating for each condition, thus reflecting changes in invasion controlled for any change in migration (Figure 4). ALOX5-BCPAP demonstrated a significant increase in invasion (50.56% ± 3.52% invasion/migration) compared to pcDNA-BCPAP cells (23.77% ± 2.63% invasion/migration). Concomitant treatment of the cells with the ALOX5 inhibitor, Zileuton, significantly reduced ALOX5-BCPAP invasion (22.65% ± 2.33% invasion/migration). Differences in invasion were statistically significant (p<0.0001). Additionally, there was no significant difference in migration between all three conditions (data not shown). Thus, increased ALOX5 expression increases cell invasion, is reversible with ALOX5 inhibition, and does not affect cell migration.

ALOX5 Activity and MMP Secretion by Protein Array and Western Blot Analysis

The influence of ALOX5 on cancer invasion has not been previously described. However, the role of ALOX5 in atherogenesis through the actions of inflammatory cells on the ECM suggest parallel mechanism in tumor pathogenesis.(Poeckel and Funk) MMPs have a central role in both ALOX5 mediated atherogenesis, and tumor invasion. (Chambers and Matrisian, 1997; Egeblad and Werb, 2002) Thus, we investigated the role of ALOX5 in MMP activity and expression in our ALOX5 transfection model of PTC. Mini protein array technology was used to assess secreted MMPs and TIMP levels in conditioned media from ALOX5-BCPAP, and pcDNA-BCPAP cells. A significantly higher level of the gelatinase, MMP-9, was detected in ALOX5-BCPAP compared to pcDNA-BCPAP. All other MMPs and TIMPS were present at relatively equal levels (Figure 5A).

To confirm the ALOX5-mediated increase in MMP-9, western blot analysis was used to determine protein levels in both SFCM from ALOX5-BCPAP cells, and in pcDNA-BCPAP

cells incubated with 0.1 μM and 1.0 μM 5-HETE, and compared to SFCM from pcDNABCPAP and pcDNA-BCPAP incubated with 10 μM AA (Figure 5B). The addition of 10 μM AA to PCDNA-BCPAP did not affect MMP-9 levels; however, the addition of 5-HETE resulted in increased MMP-9 levels in a dose dependent manner. SFCM from ALOX5-BCPAP had the highest levels of MMP-9 detected. These results corroborate the protein array data, and demonstrate that ALOX5 mediated induction of MMP-9 is 5-HETE dependent.

Concordant Expression of ALOX5 and MMP-9 in PTC and Normal Thyroid Tissue

ALOX5 expression and its metabolite 5-HETE result in increased MMP-9 protein levels *in vitro*, and suggest that there should be a correlation between ALOX5 and MMP-9 expression *in vivo*. Thus, concordant expression of ALOX5 with MMP-9 protein levels was investigated by IHC. Parallel sections of a human Thyroid/PTC tissue array were stained for ALOX5 and MMP-9 protein (Figure 6A). The mean score from two blinded, and independent pathologist are reported as 4.0±0.3(tumor) and 2.3±1.0 (normal) for MMP-9, and 4.0±0.7 (tumor) and 2.1±1.3 (normal) for ALOX5, both statistically significant when normal compared to tumor ($p<0.001$; Student t test). An MMP-9 and ALOX IHC score cut-off value of 2.5 was selected based on the mean value of normal, and samples were re-scored as "+" or "−". Chi squares analysis of this data showed a significant correlation between positive ALOX5 and MMP-9 scores ($p=0.026$, Fisher's Exact; N=42). Additionally, a linear regression of the IHC scores for ALOX5 and MMP-9 resulted in a t-value of 2.34 with a probability of 0.024, further supporting a correlation between MMP-9 and ALOX5 expression *in vivo*.

IHC analysis also provided qualitative data on protein expression in PTC (Figure 6B). Both ALOX5 and MMP-9 proteins are normally expressed in inflammatory cells. Because cancer is often associated with inflammation, it becomes important in determining if ALOX5 and MMP-9 are presently expressed by tumor cells, or infiltrating leukocytes. ALOX5 and MMP-9 were primarily localized in epithelial-derived PTC cells and exhibited diffuse cytoplasm and nuclear staining (few inflammatory cells were noted in the PTC tissue array sections (Figure 1C).

MMP-9 and ALOX5 Enhanced Invasion

The above data suggest that ALOX5 may increase PTC invasiveness through the actions of MMP-9, mediated by the ALOX5 metabolite 5-HETE. Thus the increased invasiveness of ALOX5-BCPAP may be mitigated by inhibiting MMP-9 activity. To test this, an MMP-9 inhibitory antibody and a pan-MMP inhibitor, 1,10-PE were employed in an invasion assay (Figure 7). The anti-MMP-9 antibody significantly reduced ALOX5-BCPAP invasion (from 76.26% ± 2.67 to 33.76% ± 5.92), almost to the basal invasion levels of pcDNA-BCPAP (23.34% ± 3.40%). 1,10 PE, which can inhibit all zinc dependent MMPs (and target basal invasiveness), had an even greater reduction on ALOX5-BCPAP invasion (18.75% ± 2.54). The differences in the percent invasion/migration between ALOX5-BCPAP and the other experimental condition were all statically significant ($p<0.0001$). These data support the hypothesis that ALOX5 can enhance invasion through induction of MMP-9.

Discussion

In the present study, a new paradigm for ALOX5 in tumor invasion is demonstrated by the induction of MMP-9 in PTC. Interestingly, both ALOX5 and MMP-9 genes are commonly expressed in active neutrophiles, and are involved in atherogenesis through remolding of ECM. (Poeckel and Funk) In PTC, there is also a phenomenon of ECM remodeling, which is evident in the strong desmoplastic-fibrotic response, and formation of papillary structures;

this is suggestive of an underlying inflammation-like signaling process in the tumor microenvironment. (Di Pasquale et al., 2001) Perhaps, there are some parallels between the role of ALOX5 and MMP-9 in neutrophils and aggressive cancer cells; they both migrate through, and modify the ECM, and are supported in the signaling environment of damaged tissue.

Here, increased ALOX5 is demonstrated in PTC samples compared to matched, normal tissue, and increased expression correlated to invasive histopathology features suggesting a role for ALOX5 in PTC tumor invasion. The reference controls for these expression studies were patient matched, normal-appearing thyroid tissue, taken from an area of the thyroid absent of disease. This controls for any patient specific genetic variation between normal and tumor samples, and allows for the calculation of fold induction of ALOX5 as tumor/normal tissue. While this is an ideal comparison for determining a change in expression between tumor and normal tissue, it would also be insightful to investigate the expression profile of PTC in normal thyroid tissue from healthy thyroids with no tumors. Similar studies of Cyclooxygenase-2 (a close relative of ALOX5) expression in oral squamous cell carcinoma demonstrated increased expression level in tumor and matched normal (near-adjacent tissue to the tumor) tissue, compared to normal tissue from healthy individuals, suggesting that normal tissue, adjacent to cancer in the same organ, may have an altered expression profile. (Yang et al., 2006) This may be explained by signaling factors diffusing into the normal-appearing, adjacent tissue and increasing the basal expression of these genes. Both ALOX5 and COX-2 are inducible inflammatory genes, and it is likely that they can be induced in the appropriate microenvironment. Unlike collecting oral swabs for normal oral mucosa, it would be impractical to obtain normal thyroid from healthy volunteers, as this would require a potentially harmful and invasive procedure with no benefit to the volunteer. We recognize that normal matched thyroid tissue may have higher levels of ALOX5; however, this would cause our results to be an underestimate of ALOX5 induction in PTC.

Previous investigations into the tumorigenic properties of ALOX5 in breast and prostate cancer models define its role in cell growth dynamics by affecting cell cycle and inhibiting apoptosis, but do not address tumor invasion. (Avis et al., 2001; Ghosh, 2003; Ghosh and Myers, 1997; Tong et al., 2002) Here, we conducted similar growth and survival experiments with our PTC model, and found that ALOX5 did not yielded any significant advantages. This difference in ALOX5-mediated phenotypes between PTC and other models may be explained by differences in the oncogenic background of the various tumors. Breast and prostate cancer do not typically signal through oncogenic activation of ERK, as PTC. However, 5-HETE has been demonstrated to signal through a RAS mediated, MAP-Kinase dependent ERK activation pathway, leading to cell proliferation.(Capodici et al., 1998) It is tempting to speculate that the mechanism by which ALOX5 influences proliferation and survival in breast and prostate cancer models is through this RAS/MAP/ERK pathway; although this has not been thoroughly investigated. Activation of this pathway by 5-HETE may be redundant in PTC, which already has an activation mutation in this pathway.(Melillo et al., 2005; Vasko and Saji, 2007) Up to 60% PTC is mediated through the BRAFV600E mutation, an activation mutation downstream RAS. Stimulating this pathway upstream with 5-HETE may yield no additional effects downstream; however, it may stimulate parallel pathways that originate upstream. This could explain the lack of influence ALOX5 has on proliferation and survival in our PTC model, and the induction of MMP-9. In fact, MMP-9 regulation has been linked to cell invasion via a MAP-Kinase independent pathway of RAS activation, thus supporting this hypothesis. (Bernhard et al., 1990; Gum et al., 1996; Stacey et al., 1991)

Based on our observation of increased ALOX5 expression in invasive human PTC, and supported by evidence suggesting a role for ALOX5 in ECM remodeling by active neutrophils, we investigated the role of ALOX5 in tumor invasion and MMP induction in PTC. BCPAP is a well-established BRAFV600E positive PTC cell line isolated from a human with invasive PTC, and has been characterized as a suitable model to study PTC *in vitro*.(Fabien et al., 1994) To achieve ALOX5 overexpression, a cell is required to have a permissive ALOX5 promoter and the presence of transcritptional activators such as 1,25-dihydroxyvitamin D(3) and TGFβ. (Silverman et al., 1998; Uhl et al., 2002) Initial studies demonstrated that BCPAP and other PTC and normal thyroid cells lines had relatively equivalent basal expression of ALOX5 (without the addition of any factors-data not shown). Preliminary studies also suggested that the ALOX5 promoter is hypomethylated in BCPAP cells (data not shown). ALOX5 induction by stimulating with transcriptional activators can activate multiple pathways, and make it difficult to identify the direct cause of a new phenotype. Ultimately, we decided to enhance ALOX5 expression in BCPAP by introducing an ALOX5 expression vector, and empty vector control. Although an artificial system, this method efficiently allowed us to compare two relatively similar cells with the exception of ALOX5 expression, in a PTC background. Our system sufficiently establishes a mechanistic relationship between ALOX5, invasion and MMP-9 in a BRAFV600E/ PTC background, and these experimental results were supported by our clinical findings correlating ALOX5, MMP-9 and invasive PTC. This represents a significant new finding that contributes to our understanding of how cancer cells subvert endogenous signaling mechanism in tumor pathogenesis.

In summary, this study suggests that ALOX5 can enhance invasion in PTC through a 5-HETE dependent induction of MMP-9, and demonstrates a relationship between ALOX5 and tumor invasion not been previously described. With further investigation, this new paradigm for ALOX5 in tumor pathogenesis may yield new clinical tools in diagnosing and treating PTC, and may be extended to other cancers.

Acknowledgments

Dr. Thomas Brock (Department of Internal Medicine, Division of Pulmonary and Critical Care Medicine, University of Michigan Medical School) who kindly provided us with ALOX5 expression vectors, Dr. Craig Belon (New York Medical College) for critical review, Dr. Zbigniew Darzynkiewicz (New York Medical College) for his expertise on the cell cycle and laser scanning cytometry, and Dr. Michal Schwartzman for her expertise in eicosanoids.

Financial Support

This work was supported by grants from the National Cancer Institute (1R01CA131946-01A2), and the Department of Otolaryngology, New York Medical College, Valhalla, NY USA.

References

Avis I, Hong SH, Martinez A, Moody T, Choi YH, Trepel J, Das R, Jett M, Mulshine JL. Five-lipoxygenase inhibitors can mediate apoptosis in human breast cancer cell lines through complex eicosanoid interactions. FASEB J. 2001; 15(11):2007–2009. [PubMed: 11511519]

Bednar M, Kraemer R, Abraham NG, Mullane KM. Arachidonic acid monooxygenase and lipoxygenase activities in polymorphonuclear leukocytes. Biochem Pharmacol. 1987; 36(10):1741–1747. [PubMed: 3036155]

Bernhard EJ, Muschel RJ, Hughes EN. Mr 92,000 gelatinase release correlates with the metastatic phenotype in transformed rat embryo cells. Cancer Res. 1990; 50(13):3872–3877. [PubMed: 2162246]

Bokoch GM, Reed PW. Effect of various lipoxygenase metabolites of arachidonic acid on degranulation of polymorphonuclear leukocytes. J Biol Chem. 1981; 256(11):5317–5320. [PubMed: 6787038]

Brash AR. Arachidonic acid as a bioactive molecule. J Clin Invest. 2001; 107(11):1339–1345. [PubMed: 11390413]

Capodici C, Pillinger MH, Han G, Philips MR, Weissmann G. Integrin-dependent homotypic adhesion of neutrophils. Arachidonic acid activates Raf-1/Mek/Erk via a 5-lipoxygenase-dependent pathway. J Clin Invest. 1998; 102(1):165–175. [PubMed: 9649570]

Chambers AF, Matrisian LM. Changing views of the role of matrix metalloproteinases in metastasis. J Natl Cancer Inst. 1997; 89(17):1260–1270. [PubMed: 9293916]

Di Pasquale M, Rothstein JL, Palazzo JP. Pathologic features of Hashimoto's-associated papillary thyroid carcinomas. Hum Pathol. 2001; 32(1):24–30. [PubMed: 11172291]

Ding XZ, Tong WG, Adrian TE. Multiple signal pathways are involved in the mitogenic effect of 5(S)-HETE in human pancreatic cancer. Oncology. 2003; 65(4):285–294. [PubMed: 14707447]

Egeblad M, Werb Z. New functions for the matrix metalloproteinases in cancer progression. Nat Rev Cancer. 2002; 2(3):161–174. [PubMed: 11990853]

Fabien N, Fusco A, Santoro M, Barbier Y, Dubois PM, Paulin C. Description of a human papillary thyroid carcinoma cell line. Morphologic study and expression of tumoral markers. Cancer. 1994; 73(8):2206–2212. [PubMed: 8156527]

Ghosh J. Inhibition of arachidonate 5-lipoxygenase triggers prostate cancer cell death through rapid activation of c-Jun N-terminal kinase. Biochem Biophys Res Commun. 2003; 307(2):342–349. [PubMed: 12859962]

Ghosh J, Myers CE. Arachidonic acid stimulates prostate cancer cell growth: critical role of 5-lipoxygenase. Biochem Biophys Res Commun. 1997; 235(2):418–423. [PubMed: 9199209]

Goldyne ME, Burrish GF, Poubelle P, Borgeat P. Arachidonic acid metabolism among human mononuclear leukocytes. Lipoxygenase-related pathways. J Biol Chem. 1984; 259(14):8815–8819. [PubMed: 6430891]

Gum R, Lengyel E, Juarez J, Chen JH, Sato H, Seiki M, Boyd D. Stimulation of 92-kDa gelatinase B promoter activity by ras is mitogen-activated protein kinase kinase 1-independent and requires multiple transcription factor binding sites including closely spaced PEA3/ets and AP-1 sequences. J Biol Chem. 1996; 271(18):10672–10680. [PubMed: 8631874]

Hanaka H, Shimizu T, Izumi T. Nuclear-localization-signal-dependent and nuclear-export-signal-dependent mechanisms determine the localization of 5-lipoxygenase. Biochem J. 2002; 361(Pt 3): 505–514. [PubMed: 11802780]

Jakobsson PJ, Steinhilber D, Odlander B, Radmark O, Claesson HE, Samuelsson B. On the expression and regulation of 5-lipoxygenase in human lymphocytes. Proc Natl Acad Sci U S A. 1992; 89(8): 3521–3525. [PubMed: 1314391]

Laemmli. Cleavage of structural proteins during the assembly of the head of bacteriophage T4. Nature. 1970; 227(5259):680–685. [PubMed: 5432063]

Luo M, Jones SM, Peters-Golden M, Brock TG. Nuclear localization of 5-lipoxygenase as a determinant of leukotriene B4 synthetic capacity. Proc Natl Acad Sci U S A. 2003; 100(21): 12165–12170. [PubMed: 14530386]

Luo M, Pang CW, Gerken AE, Brock TG. Multiple nuclear localization sequences allow modulation of 5-lipoxygenase nuclear import. Traffic. 2004; 5(11):847–854. [PubMed: 15479450]

Marks F, Muller-Decker K, Furstenberger G. A causal relationship between unscheduled eicosanoid signaling and tumor development: cancer chemoprevention by inhibitors of arachidonic acid metabolism. Toxicology. 2000; 153(1–3):11–26. [PubMed: 11090944]

Melillo RM, Castellone MD, Guarino V, De Falco V, Cirafici AM, Salvatore G, Caiazzo F, Basolo F, Giannini R, Kruhoffer M, Orntoft T, Fusco A, Santoro M. The RET/PTC-RAS-BRAF linear signaling cascade mediates the motile and mitogenic phenotype of thyroid cancer cells. J Clin Invest. 2005; 115(4):1068–1081. [PubMed: 15761501]

Opdenakker G, Van den Steen PE, Dubois B, Nelissen I, Van Coillie E, Masure S, Proost P, Van Damme J. Gelatinase B functions as regulator and effector in leukocyte biology. J Leukoc Biol. 2001; 69(6):851–859. [PubMed: 11404367]

Pires de Miranda M, Reading PC, Tscharke DC, Murphy BJ, Smith GL. The vaccinia virus kelch-like protein C2L affects calcium-independent adhesion to the extracellular matrix and inflammation in a murine intradermal model. J Gen Virol. 2003; 84(Pt 9):2459–2471. [PubMed: 12917467]

Poeckel D, Funk CD. The 5-lipoxygenase/leukotriene pathway in preclinical models of cardiovascular disease. Cardiovasc Res. 86(2):243–253. [PubMed: 20093252]

Randall RW, Eakins KE, Higgs GA, Salmon JA, Tateson JE. Inhibition of arachidonic acid cyclo-oxygenase and lipoxygenase activities of leukocytes by indomethacin and compound BW755C. Agents Actions. 1980; 10(6):553–555. [PubMed: 6791482]

Rasband, WS. Image J. Bethesda, Maryland, USA: National Institutes of Health; http://rsb.info.nih.gov/ij/

Ries LAG, MD.; Krapcho, M.; Stinchcomb, DG.; Howlader, N.; Horner, MJ.; Mariotto, A.; Miller, BA.; Feuer, EJ.; Altekruse, SF.; Lewis, DR.; Clegg, L.; Eisner, MP.; Reichman, M.; Edwards, BK., editors. SEER Cancer Statistics Review, 1975–2005, National Cancer Institute. Bethesda based on November 2007 SEER data submission, posted to the SEER web site, 2008. National Cancer Institute; 2008.

Roehm NW, Rodgers GH, Hatfield SM, Glasebrook AL. An improved colorimetric assay for cell proliferation and viability utilizing the tetrazolium salt XTT. J Immunol Methods. 1991; 142(2): 257–265. [PubMed: 1919029]

Sato H, Takino T, Okada Y, Cao J, Shinagawa A, Yamamoto E, Seiki M. A matrix metalloproteinase expressed on the surface of invasive tumour cells. Nature. 1994; 370(6484):61–65. [PubMed: 8015608]

Silverman ES, Du J, De Sanctis GT, Radmark O, Samuelsson B, Drazen JM, Collins T. Egr-1 and Sp1 interact functionally with the 5-lipoxygenase promoter and its naturally occurring mutants. Am J Respir Cell Mol Biol. 1998; 19(2):316–323. [PubMed: 9698605]

Soumaoro LT, Iida S, Uetake H, Ishiguro M, Takagi Y, Higuchi T, Yasuno M, Enomoto M, Sugihara K. Expression of 5-lipoxygenase in human colorectal cancer. World J Gastroenterol. 2006; 12(39): 6355–6360. [PubMed: 17072961]

Stacey DW, Roudebush M, Day R, Mosser SD, Gibbs JB, Feig LA. Dominant inhibitory Ras mutants demonstrate the requirement for Ras activity in the action of tyrosine kinase oncogenes. Oncogene. 1991; 6(12):2297–2304. [PubMed: 1766676]

Stuve O, Dooley NP, Uhm JH, Antel JP, Francis GS, Williams G, Yong VW. Interferon beta-1b decreases the migration of T lymphocytes in vitro: effects on matrix metalloproteinase-9. Ann Neurol. 1996; 40(6):853–863. [PubMed: 9007090]

Tong WG, Ding XZ, Adrian TE. The mechanisms of lipoxygenase inhibitor-induced apoptosis in human breast cancer cells. Biochem Biophys Res Commun. 2002; 296(4):942–948. [PubMed: 12200139]

Uhl J, Klan N, Rose M, Entian KD, Werz O, Steinhilber D. The 5-lipoxygenase promoter is regulated by DNA methylation. J Biol Chem. 2002; 277(6):4374–4379. [PubMed: 11706027]

Vasko VV, Saji M. Molecular mechanisms involved in differentiated thyroid cancer invasion and metastasis. Curr Opin Oncol. 2007; 19(1):11–17. [PubMed: 17133106]

Westermarck J, Kahari VM. Regulation of matrix metalloproteinase expression in tumor invasion. FASEB J. 1999; 13(8):781–792. [PubMed: 10224222]

Yang P, Chan D, Felix E, Madden T, Klein RD, Shureiqi I, Chen X, Dannenberg AJ, Newman RA. Determination of endogenous tissue inflammation profiles by LC/MS/MS: COX- and LOX-derived bioactive lipids. Prostaglandins Leukot Essent Fatty Acids. 2006; 75(6):385–395. [PubMed: 17011176]

Zeng ZZ, Yellaturu CR, Neeli I, Rao GN. 5(S)-hydroxyeicosatetraenoic acid stimulates DNA synthesis in human microvascular endothelial cells via activation of Jak/STAT and phosphatidylinositol 3-kinase/Akt signaling, leading to induction of expression of basic fibroblast growth factor 2. J Biol Chem. 2002; 277(43):41213–41219. [PubMed: 12193593]

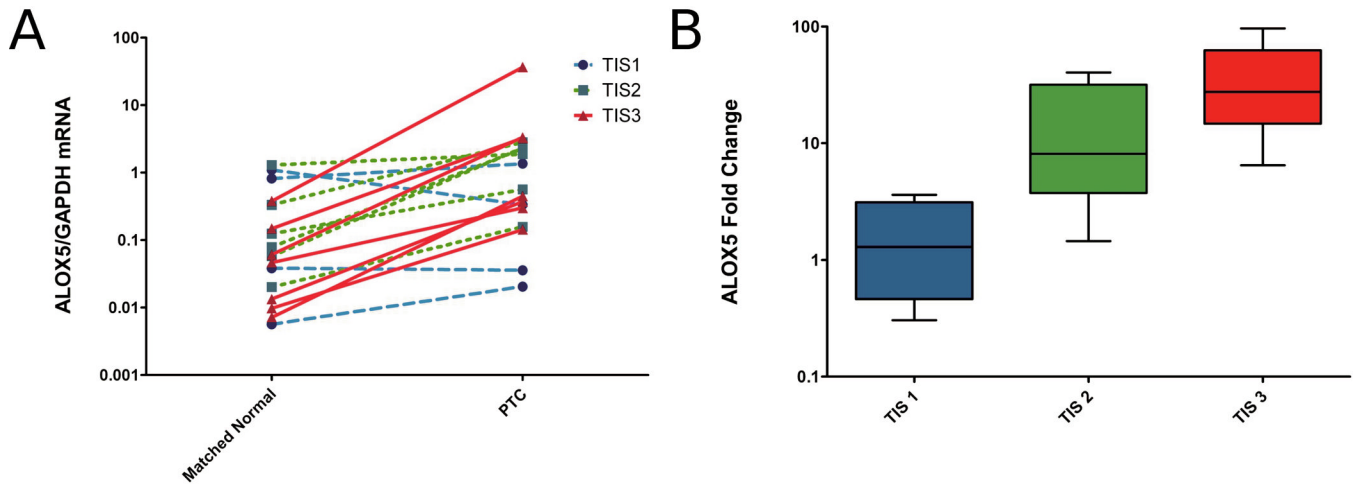

Figure 1.

ALOX5 mRNA expression correlates with tumor invasiveness. (A) GAPDH normalized ALOX5 expression in 17 pairs of PTC and patient-matched, normal thyroid tissue measured by quantitative real-time RT-PCR. Data points represent average values of samples run in triplicate, lines link tumor and patient-matched, normal thyroid pairs, and colored line depicts TIS value (blue=TIS1, green=TIS2, red=TIS3). Mean ALOX5/GAPDH mRNA for patient-matched, normal samples is 0.27±0.10, and for PTC is 3.291±2.089; p =0.0024 (Wilcoxon signed rank test). (B) Box plot of the tumor-to-normal fold difference in ALOX5 expression stratified by TIS, demonstrate a positive Spearman correlation (r_s=0.74, p= 0.0007; TIS1 n=4, TIS2 n=5, TIS3 n=8).

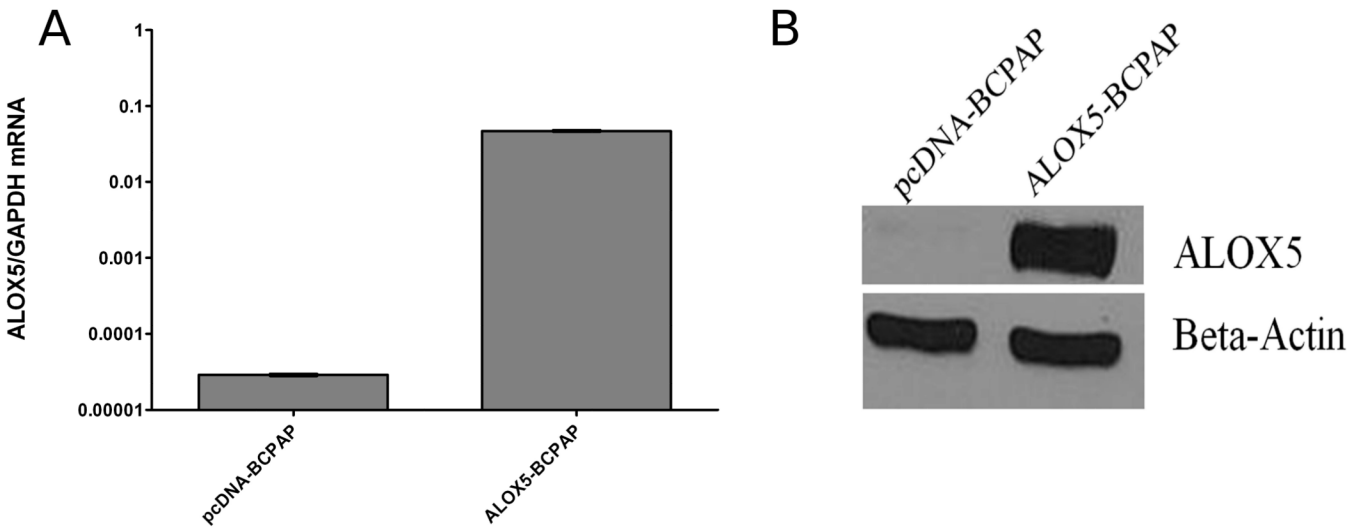

Figure 2.

Validation of ALOX5-BCPAP and pcDNA-BCPAP transfectants by quantitative real-time RT-PCR for ALOX5 mRNA (A), and western blot analysis for ALOX5 protein (B). (A) Mean ALOX5 expression increased 156 fold in transfected cells.

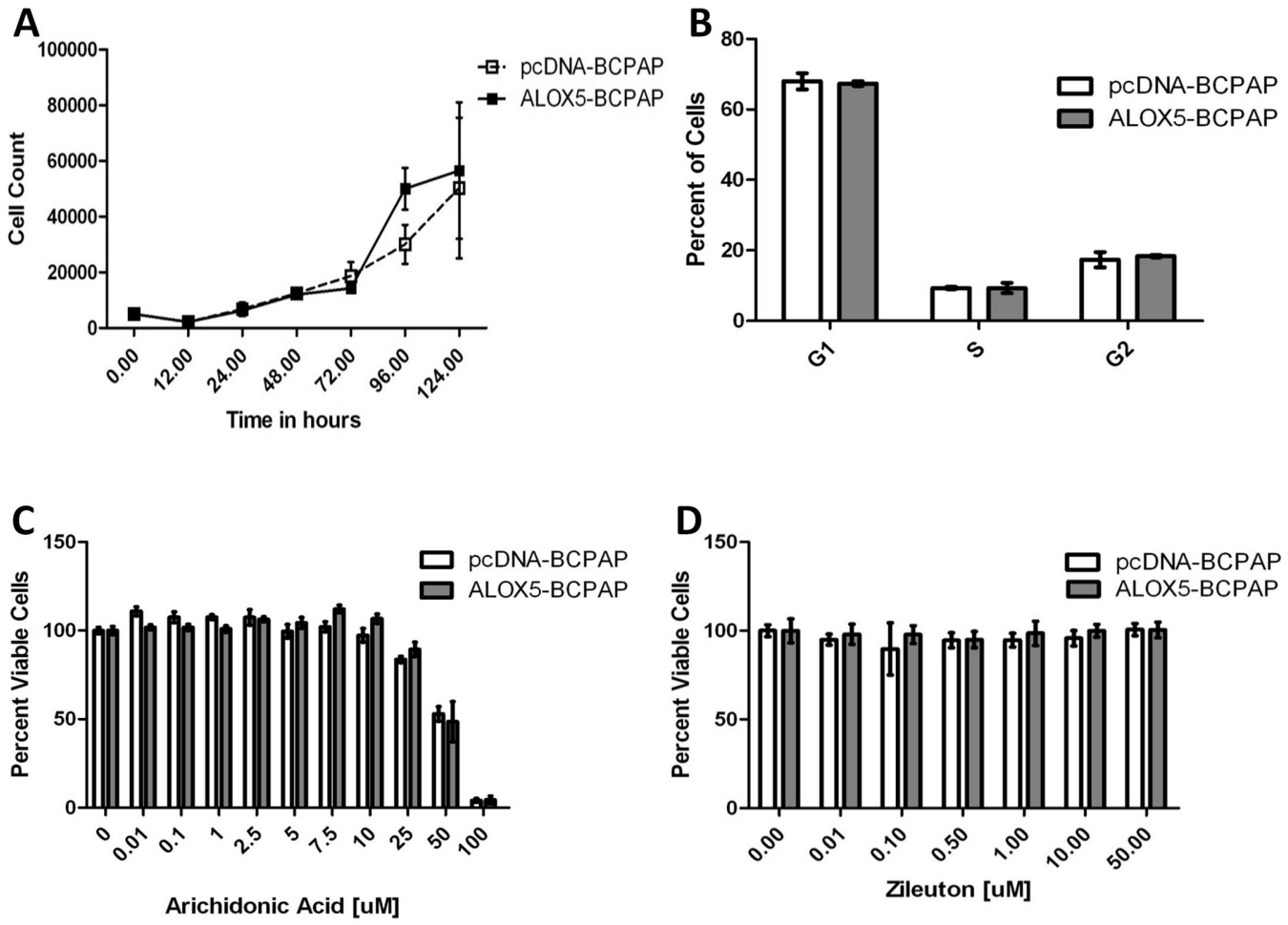

Figure 3.

ALOX5 expression and activity under normal culture conditions. (A) Growth curves were generated for ALOX5-BCPAP and pcDNA-BCPAP under standard conditions by trypan-blue exclusion. (B) Ten-thousands cells per condition were grown to 50% confluence and cell cycle was assessed by laser scanning cytometry. (C) The dose dependent effects of arachidonic acid (C) and Zileuton (D) on cell viability were determined by XTT metabolism. Twenty-five thousand cells were plated in replicates of 6 for each condition and cell viability was measured at 72 hours post treatment; error bars represent standard deviation.

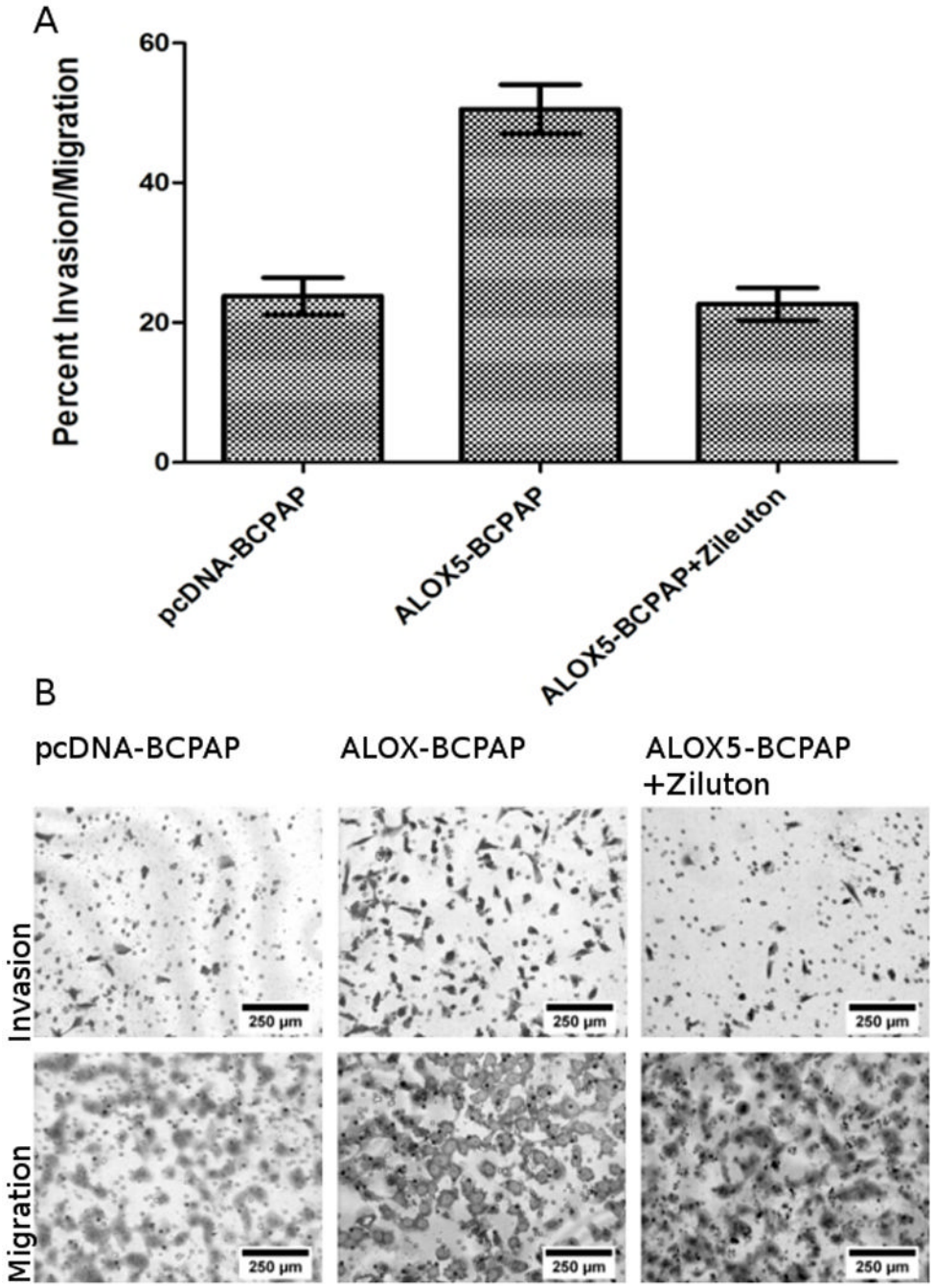

Figure 4.

ALOX5 promotes invasion across a Matrigel barrier. Fifteen thousand ALOX5-BCPAP±50 μM Zileuton, and pcDNA-BCPAP (empty vector control) were incubated in quadruplicate on ECM coated (invasion) or non-coated (migration) Boyden chambers. Cell were allowed to invade and migrated towards 10% FBS supplemented RPMI for 22 hours followed by quantification. (A) Mean values for percent invasion/migration for each conditions are: pcDNA-BCPAP = 23.77%±2.63, ALOX5-BCPAP = 50.56% ±3.52, ALOX5-BCPAP + 50 μM Zileuton mean = 22.65±2.33. ALOX5-BCPAP was significantly more invasive than the other two conditions (p<0.0001, t-test). (B) Representative photomicrographs of invasion and migration chambers at 100X magnification.

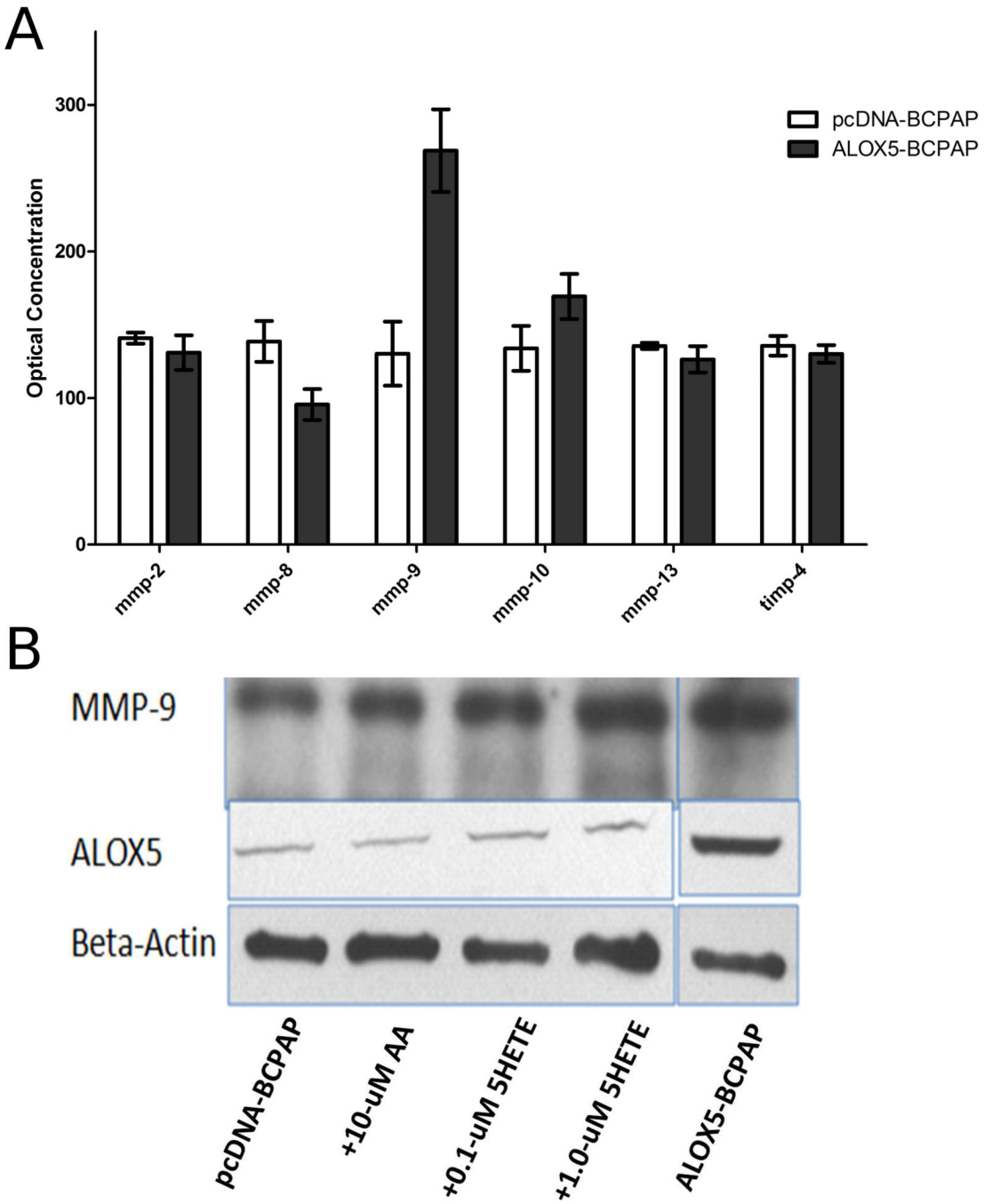

Figure 5.

MMP-9 levels in BCPAP conditioned media in response to ALOX5 gene transfection and exogenous 5-HETE. (A) Conditioned media were prepared from 100,000 pcDNA-BCPAP and ALOX5-BCPAP cells cultured, in duplicate, and MMP protein levels were assessed using the RayBio Human Matrix Metalloproteinases Antibody Array. ALOX5-BCPAP has significantly higher levels of MMP-9 compared to pcDNA-BCPAP (p=0.032, t-test). (B) 5-HETE and ALOX5 increase MMP-9 levels in conditioned media, determined by western blot analysis.

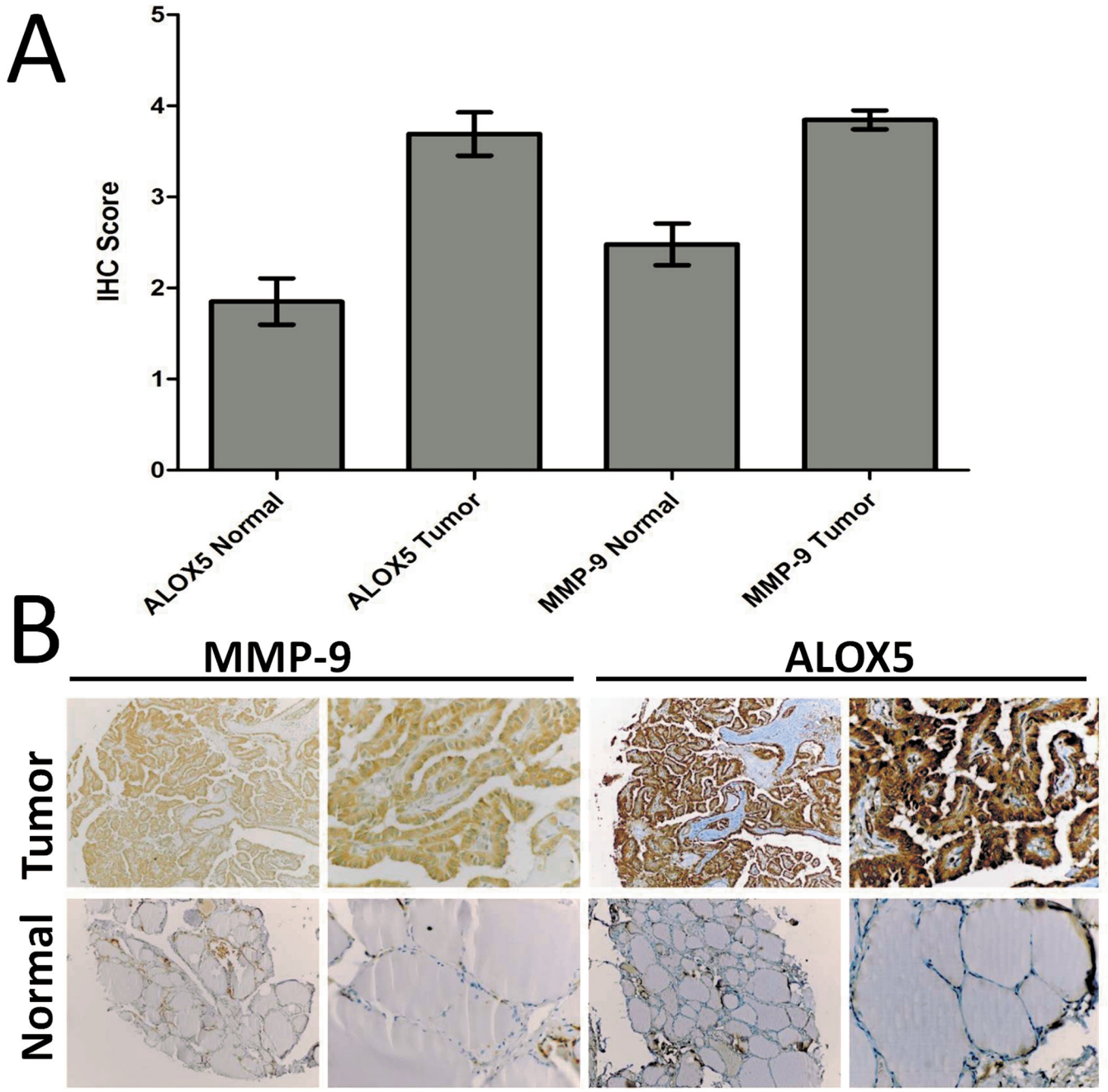

Figure 6.

ALOX5 and MMP-9 IHC in parallel sections of a human Thyroid and PTC tissue array demonstrate concordant protein expression. (A) Bar graphs representing the mean IHC score from two independent pathologist, Tumor =4.0±0.7 for ALOX5 and 4.0±0.3 for MMP-9 Normal=2.1±1.3 and 2.3±1.0 for MMP-9 (Tumor vs. Normal: $p<0.001$ Student t test for both). (B) Representative IHC section of the 20 cancer and 26 normal-appearing thyroid tissues.

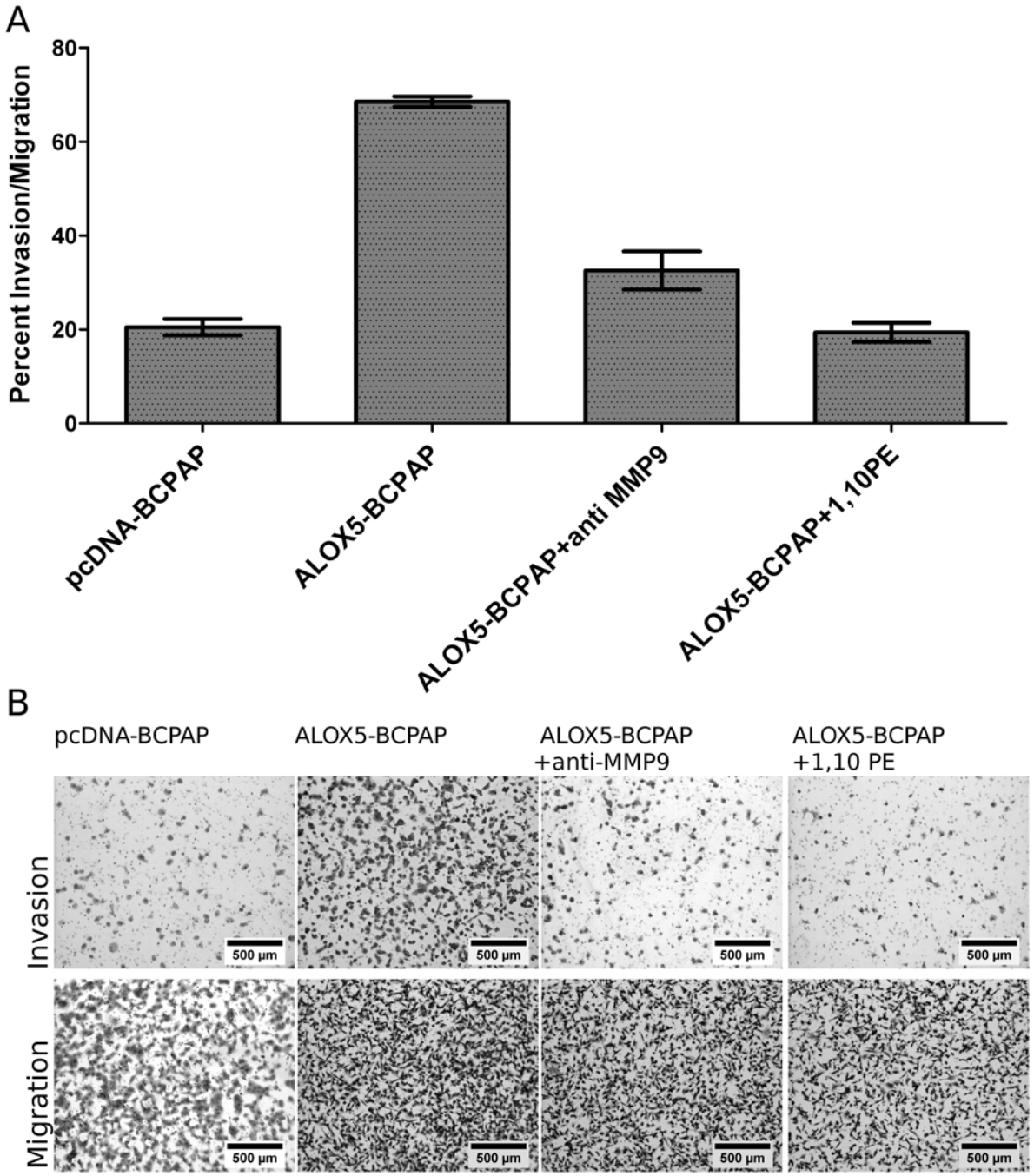

Figure 7.

MMP-9 inhibition abrogates ALOX5 induced invasion in BCPAP cells. For each condition, 25,000 cells were plated in quadruplicate on ECM coated (invasion) or non-coated Boyden chambers. Cell were allowed to invade and migrate towards 5% FBS supplemented RPMI for 22 hours followed by quantification. (A) Data represented as the mean percent invasion/migration; pcDNA-BCPAP=23.34±2.48; ALOX5-BCPAP=76.26±2.67; ALOX5-BCPAP + anti MMP9=33.76±5.92; ALOX5-BCPAP + 1,10 PE=18.75±2.54. Invasion was significantly increased only in ALOX5-BCPAP compared to pcDNA-BCPAP (p<0.0001, t-test). (B) Representative photomicrographs of invasion and migration chambers at 50X magnification.

Table 1

Characteristics of patient samples. TIS score is based on invasive histopathological features, TIS-1 = no evidence of invasive disease, TIS-2 = evidence of lymph node involvement and/or capsule involvement, TIS-3 = extra thyroid extension and/or regional spread.

Age	Sex	Size	Multifocal	TNM	Stage	TIS	BRAFV600E Genotype	ALOX5 T/N mRNA
55	M	2.1cm	Y	T3NxMx	III	3	V600E	96.08
23	F	3.4cm	N	T3NxMx	I	3	V600E	63.47
39	F	1.1cm	N	T3N1aMx	I	3	V600E	54.04
74	F	2.3cm	Y	T3NxMx	III	3	WT	40.46
41	F	1.3cm	Y	T3N1bMx	I	3	V600E	27.48
74	F	3.0 cm	Y	T4aN1M0	III	3	WT	21.82
52	M	0.9cm	Y	T3N1aMx	III	3	V600E	14.7
45	F	1.7 cm	Y	T3N1bMx	III	3	WT	6.46
49	F	1.2cm	Y	T3NxMx	III	2	WT	28.74
61	F	2.8cm	Y	T3NxMx	III	2	WT	8.52
36	F	2.6cm	Y	T2NxMx	I	2	V600E	7.78
54	F	1.5 cm	N	T3NXM0	III	2	WT	4.54
31	M	1.7cm	N	T1NxMx	I	2	V600E	1.46
25	F	2.5cm	N	T2NxMx	I	1	V600E	3.61
37	F	2.0cm	Y	T1NxMx	I	1	WT	1.66
68	F	2.5cm	Y	T2NxMx	II	1	WT	0.93
63	F	2.1 cm	Y	T2NXM0	I	1	WT	0.31